SUPPLEMENTAL MATERIALS AND METHODS

Supplemental Figure 1. *Fasciclin* family expression in E10.5 hearts. (A) *Periostin*, **(B)** *βigH3* and **(C)** *stabilin-1* expression analysis via *in situ* hybridization. Both *periostin* and *βigH3* are co-expressed in cardiac fibroblasts almost as soon as they first appear in mammalian embryonic heart (arrows in A & B). Transmembrane *stabilin-1* gene is expressed in adjacent endothelial lineage (C). Note while *periostin* is confined to endocardial cushion cells of OFT, *βigH3* is expressed in both OFT cushions and adjacent myocardial cuff. Both sense and anti-sense [^{35}S]UTP-radiolabeled RNA probes were transcribed and used for *in situ* hybridization on at least 6-8 mouse embryos at each stage using established techniques[1,2]. Specific signal was only observed when sections were hybridized with the anti-sense probe.

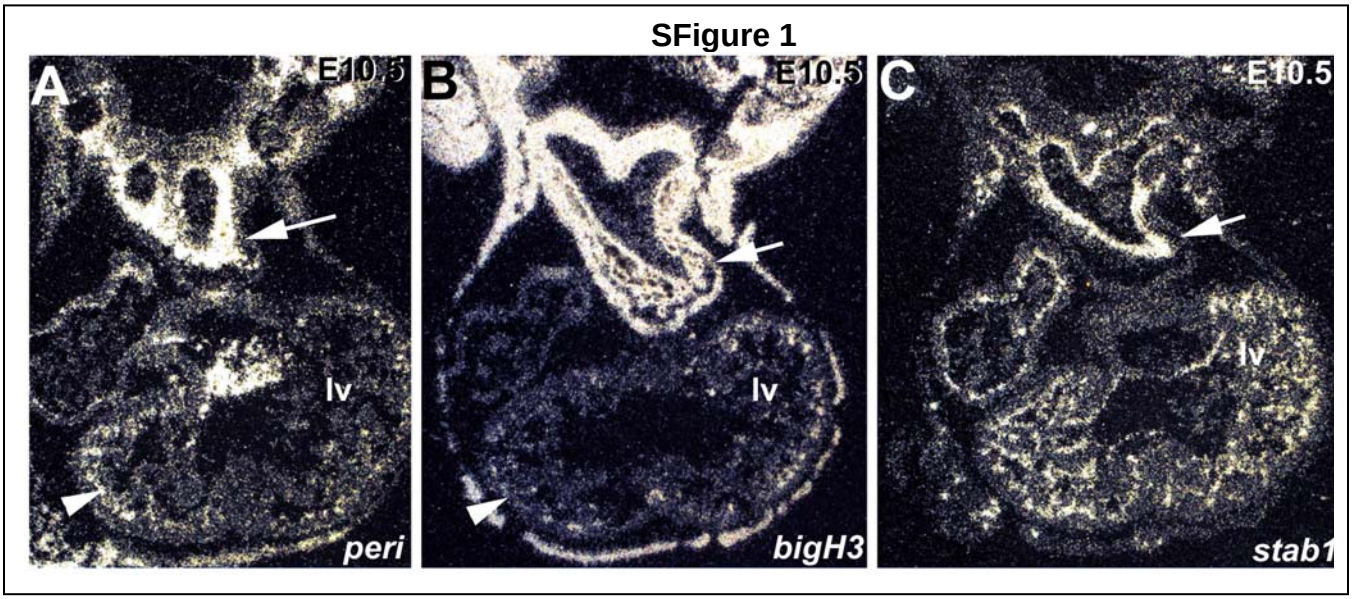

Supplemental Figure 2. Periostin protein localization in early heart. Immunohistochemistry reveals periostin is expressed in E10 **(A,B)** endocardial cushions and is co-localized with cardiac jelly matrix and both OFT and AV mesenchymal cushion cells, but is absent from endothelium and adjacent cardiomyocytes. In E11.5 cushions **(C,D)**, periostin protein becomes restricted to cushions cells that abut the adjacent myocardium. Note punctuate expression in cardiac fibroblasts and within epicardium (arrow in C). Periostin is robustly expressed in both the E13 aortic valve leaflets and valvular attachment apparatus (arrow in **E**), as well as the mitral valve leaflets **(F).** Immunostaining of periostin (1:10,000

dilution) using the ABC kit (Vector) following manufacturer's directions, was performed as described[3]. Negative controls that lacked either the primary or secondary or both did not produce any DAB staining (not shown).

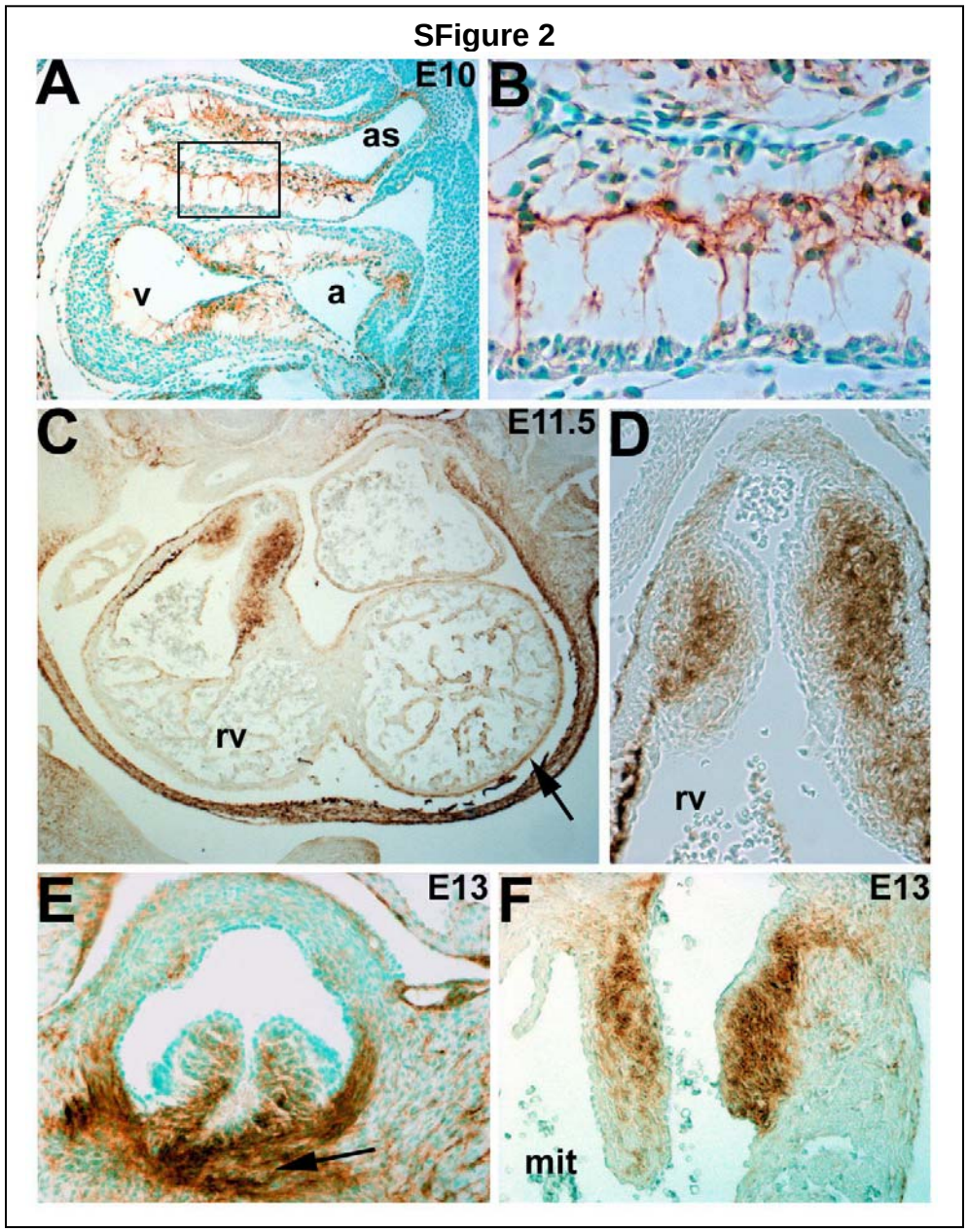

Supplemental Figure 3. Elevated periostin in failing hearts is confined to cardiac fibroblast lineage. To assess the pathological responses of periostin, we examined periostin responses to pressure overload, fibrosis and myocarditis. Acute LV pressure overload was created by microsurgical transverse aortic constriction[4]. At 2 and 7 days post-surgery, constricted and sham-operated heart were removed and LV weight determined. The LV weight

was indexed to body weight to verify expected heart weight increase in only the 7-day constricted animals[4]. Adult hearts were then perfusion-fixed with phosphate buffered saline (PBS)/4% PFA and dissected to enable morphometric and marker analysis as wholemounts and histological sections. Heart samples were harvested, fixed, sectioned (6μm), stained with hematoxylin and eosin (H&E for cardiac histology), Sirius red/Fast green (for potential cardiac fibrosis), von Kossa (detect calcification), and Resorcin-Fuchsin/van Gieson (stain collagen & elastin fibers).

Significantly, in ventricular samples that had been subjected to acute LV pressure overload, the ~85, 87 and 90kDa periostin isoforms are upregulated specifically within cardiac fibroblasts 7 days after banding (64x fold). Protein levels were normalized by amido black staining (n=4 banded LV and 4 sham-operated LV pooled samples; scale bars: 50μm). Perisotin is upregulated (64x) in banded samples 7 days post-surgery and coincident with development of fibrous (SFig. 3A). However, periostin is unchanged in banded hearts 2 days post-surgery (not shown). Furthermore, spaciotemporal upregulation is only observed in the cardiac fibroblast lineage and in regions of overt fibrosus (SFig. 3D & E). These findings are consistent with microarray results that profiled genetic responses during infarction[5], and indicate upregulation is within the cardiac fibroblast lineage occurring within 1-week of infarction. **(B & D)** Cryostat sections through ventricles of 7day banded adult heart. B & D panels show sections, stained with Sirius red (stains fibrotic regions) and fast green (stains cardiomyocytes). Note fibrosis and abundant collagen deposition (red signal) throughout the banded heart. **(C & E)** Adjacent sections stained for periostin protein expression (brown DAB staining). Note up-regulation of expression in only cardiac fibroblasts in banded failing hearts.

Given the robust periostin upregulation observed in response to aortic banding, we assessed the spatiotemporal expression of periostin in a myocarditis model – namely DBA/2 inbred mice (SFig. 3F-H). DBA/2 mice spontaneously develop myocarditis and a unique form of subepicardial inflammation of the right ventricle characterized by a prominent eosinophilic infiltrate with calcinosis[6]. The myocardial injury is most severe ~7 weeks but heals with myocardial fibrosis and calcinosis ~10 days later. Western analysis revealed periostin levels were unchanged in 4-week DBA/2 hearts prior to myocarditis but significantly increased (23x fold) in 8-week fibrotic hearts (not shown). Immunohistochemistry revealed periostin upregulation is most evident in the fibrotic regions, surrounding calcified nodules but absent

from the cardiomyoctes. Analysis of 7-week DBA/2 hearts exhibiting myocardial fibrosis, necrosis and calcinosis revealed that upregulated periostin expression is confined to the regions of calcification, restricted to the activated cardiac fibroblasts and is also absent from cardiomyocytes (SFig. 3F-H). **(F)** von Kossa staining shows subepicardial mineralization (black), while **(G)** Sirius red indicates fibrosis at site of myocardial injury. Note periostin (brown DAB staining) immuno-detection **(H)** demonstrates that periostin expression overlaps region of calcification and is restricted to the activated cardiac fibroblasts. (n=5 hearts examined). Our data, and that shown by Molkentin et al.[5] and Markwald et al.[7] clearly demonstrate that periostin is not expressed in cardiomyocytes in either the normal, failing and/or dilated mice hearts. Thus, despite both acute LV pressure overload and myocarditis causing significant ventricular fibrosis, abundant collagen deposition and significant periostin upregulation; periostin expression is confined to the cardiac skeleton and valves,

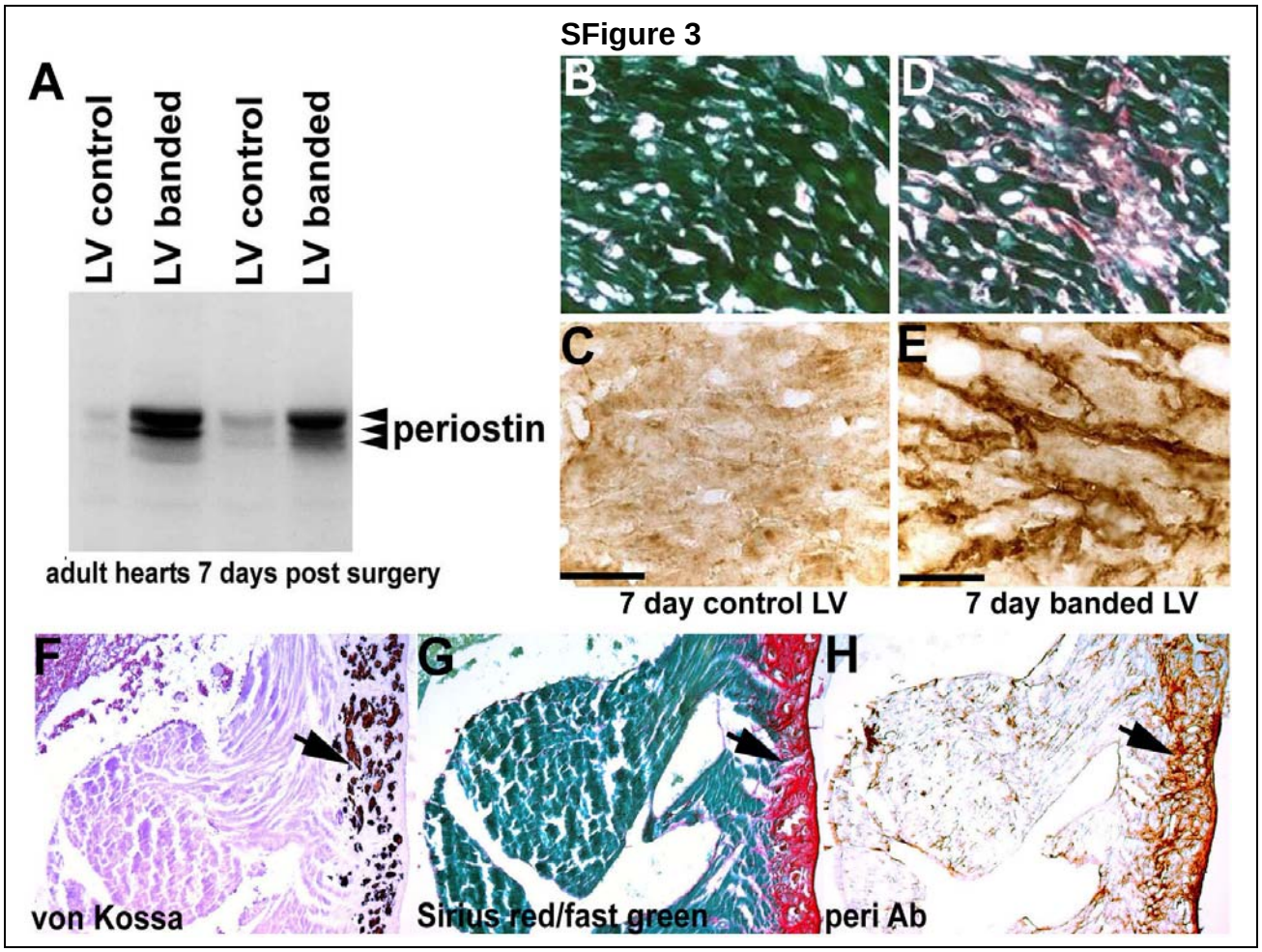

Viable *peri*^{lacZ} valve annuli and leaflets are hypoplastic: Histology reveals 100% of null (n=8/8 sectioned) mitral and tricuspid leaflets are significantly shorter (relative lengths indicated by green dotted line in H&E sections; wildtype=2,232μm+/-18μm vs. null=1,306μm+/-51μm; P<0.05) and thickened compared to wildtype littermates (Fig. 3b). Subsequent analysis of proliferation index and cell density in wildtype and *peri*^{lacZ} null littermates containing the *αMHC-EGFP* reporter, indicate null cushions are initially formed normally, and exhibit equivalent proliferation and have similar cell densities, compared to wildtypes. When DAPI-positive EGFP-negative nuclei, that stained positively for BrdU, were compared in E14 cushions (n=4; +/+ was 12.4+/-0.5%; *peri*^{lacZ} null was 11.2+/-4%), newborn (n=3; +/+ was 1.7+/-0.8%; *peri*^{lacZ} null was 1.9+/-3%) and four month leaflets (n=3; +/+ was 0.06+/-0.01%; *peri*^{lacZ} null was 0.043+/-0.007%), there were no statistically significant differences. As normal adult cardiomyocytes have a labeling index of ~0.0005%[8], the more than 100-fold higher proliferative index suggests postnatal valves remain active, dynamic structures. Furthermore, histomorphometric analysis of four month old *peri*^{lacZ} null and littermate control hearts (n=6 of each genotype), revealed that DAPI-positive, but EGFP-negative fibroblast cell numbers were unaffected by loss of *periostin* (+/+ fibroblast content was 81.4+/-2.8% of total cells, n=2,657 cells; and *peri*^{lacZ} null fibroblast content was 74.7+/-1.65% of total cells, n=3,431 cells counted). Similarly, total cellularity of four month old wildtype ventricle was 1,224 cells/1,4mm^2 (n=6) and *peri*^{lacZ} null was 1,127 cells/1,4mm^2 (n=6), indicating no significant differences in global cell number, despite systemic periostin loss.

Supplemental Figure 4. Mesenchymal cushion differentiation is perturbed in absence of Periostin. To visualize the cardiac skeleton, we made use of the *αMHC-EGFP* reporter mice to distinguish EGFP-positive cardiac myocytes from other cell types in the mature heart. Significantly, the adult surviving *peri*^{lacZ} null short leaflets contained ectopic islands of *αMHC-EGFP* cardiomyocytes, as isolated EGFP-positive cells are present in null mitral and tricuspid leaflets (SFig. 4). Similarly, ectopic αSMA-expression is also present in adult null valves. **(A-C)** Phase (A) and EGFP (B&C and inset) images of 4-month adult wildtype (A&B) and *peri*^{lacZ} null (C & enlarged inset) hearts containing the *αMHC-EGFP* transgenic reporter. Note ectopic EGFP-positive myocyte islands are present in null valves (n=9/13 *peri*^{lacZ} null *αMHC-EGFP* hearts examined). (D,E) αSMA expression in wildtype (D) and *peri*^{lacZ} null (E & enlarged

inset). Note ectopic actin-expressing clusters in short null leaflets (arrow in inset; n=3/13 *peri*^{lacZ} null *αMHC-EGFP* hearts examined).

SFigure 4

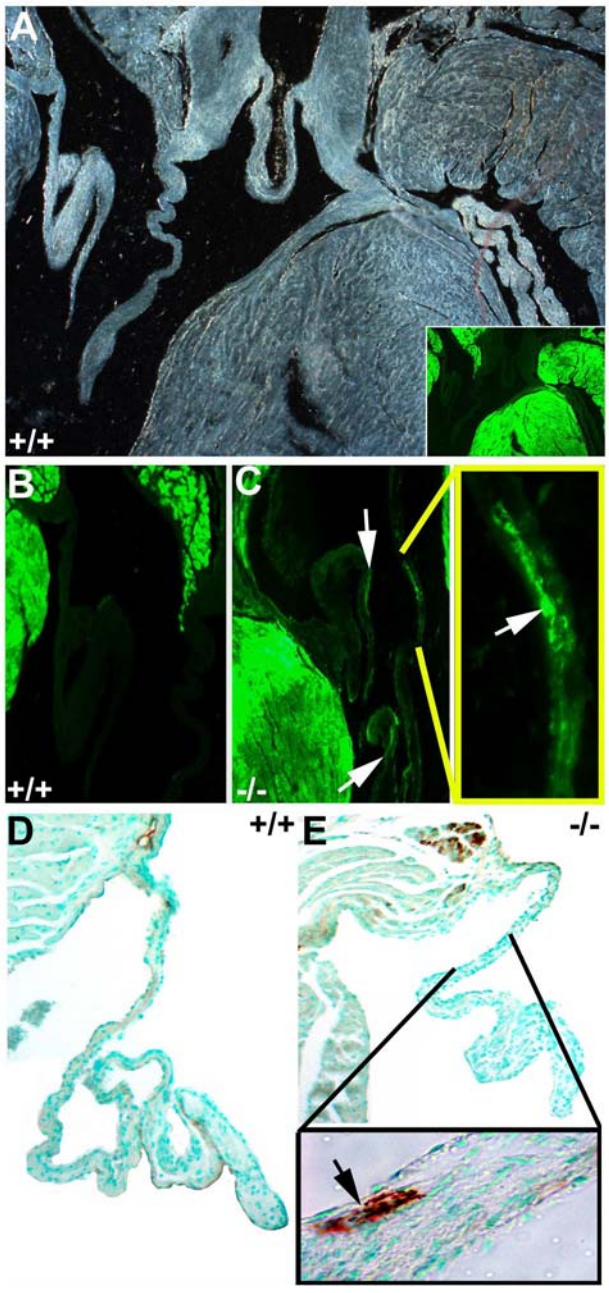

Supplemental Figure 5. 3D-collagen lattice formation results. Collagen gel contraction assays were employed specifically to quantitatively examine the effect of periostin on alignment and condensation of pre-existing fibrils analogous to what might be occurring *in* vivo when cushions become attenuated into cusps by the compactions and organization of fibrils and other ECM components into stratified layers of dense regular fibrous tissue – rather than study fibrillogenesis itself. This assay enables us to assess the mechanism and function and significance of periostin binding to collagen. To evaluate the ability of fibroblasts to reorganize and contract 3D-collagen lattices and their response to exogenously added TGFβ, wildtype and *peri*^{lacZ} null E14 MEFs were cast into floating collagen lattices, and daily contraction measured, as previously described[9,10]. Similarly, TGFβ responses of wildtype and *peri*^{lacZ} null E14 MEF lines were also compared.

Whilst wildtype collagen lattices rapidly contracted from a starting diameter of 3.5cm to less than 2cm over 5 days, the *peri*^{lacZ} null fibroblasts exhibit reduced reorganization and contraction ability (SFig. 5). The average degree of contraction in 3 independent cell lines per genotype (measured as the gel area as a percentage of the original area) for wildtype MEFs was 42% (day1), 78% (day2), 84% (day3) 91% (day4) 100% (day 5); while the mutant was

12% (day1), 20% (day2), 33% (day3) 52% (day4) 52% (day 5). Similarly, when wildtype lattices were exposed to increasing TGFβ (0.1 and 1ng/ml) they contracted significantly more than untreated lattices cultured for the same length of time. When lattices seeded with *peri*^{lacZ} null MEFs were compared with wildtype in the presence of exogenously added 0.1 or 1ng/ml TGFβ (SFig. 5), the *peri*^{lacZ} null fibroblasts exhibit reduced reorganization and contraction ability (null gels were ~51% larger than wildtype gels; for all gel contraction experiments $P<0.05$ was considered statistically significant). This supports the hypothesis that loss of *periostin* results in a blunted TGFβ ECM response.

SFigure 5

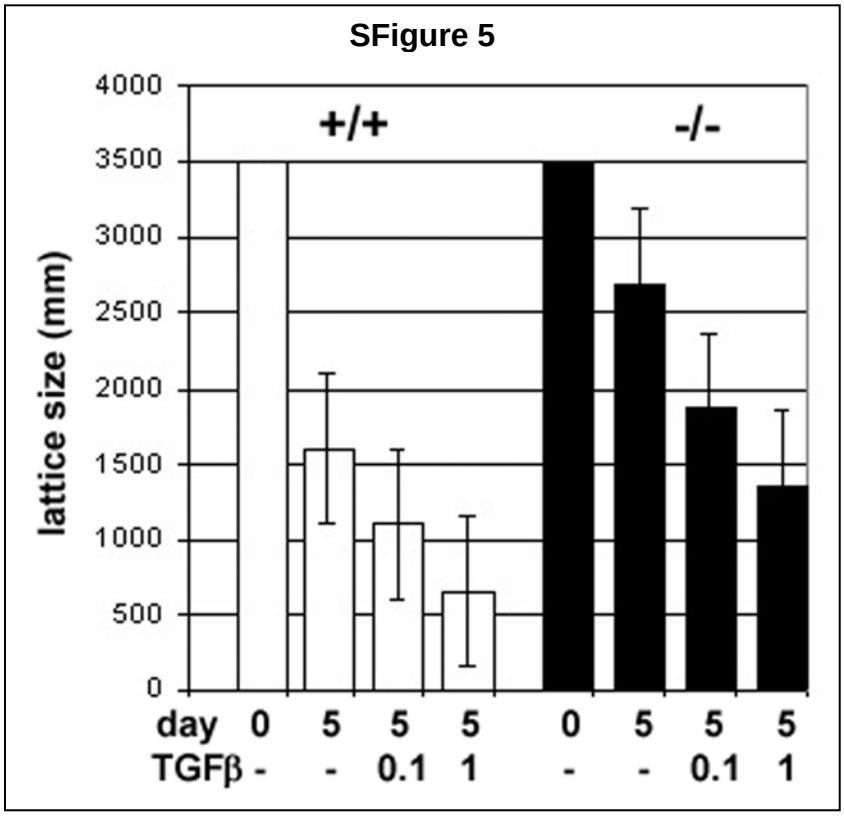

METHODS:

Animal models: *Periostin* (*peri*^{lacZ}) knockin knockout mice generated previously were maintained on a C57BL/6J genetic background and fed powdered Teklad LM-485 Complete Mouse Diet to alleviate runting[11]. *Peri*^{lacZ} mice were intercrossed with *αMHC-EGFP* reporter mice[12] that express EGFP under the control of the cardiomyocyte-restricted αmyosin heavy chain (αMHC) promoter. To assess TGFβ responsiveness, periostin expression was measured in *αMHC-TGFβ1* mice[13], that express constitutively active mutant TGFβ1 cys33ser. To assess

the pathological responses of periostin, acute left ventricular (LV) pressure overload and sham-operated control samples were created by microsurgical transverse aortic constriction as described previously[4]. Adult DBA/2 inbred mice that spontaneously develop myocarditis[6] were purchased from Jackson Laboratories and periostin examined. All animal experimentation was performed in accordance with National Institutes of Health Guidelines, and protocols approved by the Institutional Animal Care and Use Committee at IUPUI.

Histological, in situ, RT-PCR and immunohistochemical analysis: Tissue isolation, fixation and processing for *lacZ* staining was carried out as described[11]. Histomorphometric and proliferation analysis of *peri*^{lacZ} hearts are standard and detailed in supplement. Sections (12μm) and microdissected tissues were subjected to S^{35} *in situ* hybridization and immunohistochemical analyses of matrix-bound and secreted periostin was carried out as described[1,2,5,11]. Pediatric aortic valve tissue was obtained as described[13]. Resorcin-Fuchsin/vanGieson staining was used to detect collagen/elastin and alcian blue (pH2.5) to detect glycosaminoglycans; and αSMA (Sigma), collagen-I (SouthernBiotech), Ddr2 (Santa Cruz), MF20 (Hybridoma bank), and αsarcomeric actin (Sigma) antibodies were used to assess lineage-restricted periostin expression. Phospho-Smad2,3 antibody (Cell Signaling) was used to assess Tgfβ signaling.

Histomorphometric and proliferation analysis: Four month old *peri*^{lacZ} null and age matched littermate control hearts containing the α*MHC-EGFP* reporter were serially sectioned (6μm) and stained with 4',6-diamidino-2 phenylindole (DAPI) to demonstrate nuclei via fluorescence microscopy (n=6 hearts/genotype). Histomorphometric analysis was performed on digital images (via ImageJ software, NIH) to assess relative cardiac fibroblast cell numbers and total ventricular cellularity. EGFP-positive cells containing DAPI nuclei and total DAPI stained nuclei were counted from 4 random fields (at 200x mag) per slide and 2 slides/ventricle. Leaflet lengths were measured between the anchoring point to the annulus fibrosus and the free edge as described[14]. Valvular attachment site areas were determined via measurement of the DAPI stained and α*MHC-EGFP* negative area using combined phase/fluorescence microscopy. Incorporated (BrdU at 1ml/100g, ZYMED) immunopositive cells/compared to DAPI-stained

total, were counted from 4 random fields (200x mag) per slide and 2 slides/heart, with total of 6 hearts per group for statistically testable analyses.

Isolation and Culture of Cells: For TGFβ-responsiveness studies, wildtype and *peri*^{lacZ} null cardiomyocytes and fibroblasts were obtained from collagenase digestion of E14 and newborn hearts, as described for neonatal hearts[15] except digestion times were reduced for fetal hearts. Fibroblasts were separated from myocytes by selective cellular attachment, and myocytes were further purified by using a Percoll density gradient (Sigma). Fibroblasts were cultured in Dulbecco's modified Eagle medium (DMEM; Gibco) supplemented with 10% NBS, 5% FCS, 1% penicillin/streptomycin (Sigma). Myocytes were maintained in DMEM containing 8% horse serum (Gibco), 5% NBS, 1% penicillin/streptomycin. Cardiac fibroblasts and myocytes were cultured alone or co-incubated with TGFβ (1ng/ml; Gibco) for 16hrs, and used for RT-PCR as described[1,2,11].

MEFs were isolated from wildtype and *peri*^{lacZ} null E14 embryos, and used to assess collagen production and 3D-lattice formation ability, using the methods described[9,10]. Collagen production by wildtype and *peri*^{lacZ} null MEFs alone or co-incubated with TGFβ(1ng/ml; Gibco) in 24-well tissue culture plates was assessed by [^{3}H]proline incorporation. Equivalent MEFs (10^5 cells from 3 independent cell lines per genotype) were assessed as described[10].

For assessment of 3D-lattice formation ability, collagen type-I from rat tail tendon (2mg/ml in 18mM acetic acid) was added to 35mm dishes containing DMEM, 1% pen/strep with 1% FCS and 0.1M NaOH. Wildtype and *peri*^{lacZ} null MEFs (10^5 cells/well) were added just after collagen solution, before fibrillation and lattice formation. The relaxed, free-floating gels were incubated at 37°C and the media (+/- 0.1 and 1ng/ml TGFβ) changed daily. The lattices were photographed and rates of gel contraction were calculated by determining the remaining surface area by computer-based analysis and expressed as either percentage of initial area or percentage of control area. Data are presented graphically as mean +/-sd. Lattice area was statistically compared with Student's *t* test. Significant differences were determined at $P<0.05$.

Literature cited:

1. Kruzynska-Frejtag A, Machnicki M, Rogers R, Markwald RR, Conway SJ. Periostin is expressed in the embryonic mouse heart during valve formation. *MOD*, 2001;103:183-188.
2. Lindsley A, Li W, Wang J, Maeda N, Rogers R, Conway SJ. Comparison of four mouse fasciclin-containing genes expression patterns during valvuloseptal morphogenesis. *Gene Expr Patterns*. 2005;5:593-600.
3. Kanekar S, Borg TK, Terracio L, Carver W. Modulation of heart fibroblast migration and collagen gel contraction by IGF-I. *Cell Adhes Commun.* 2000;7:513-23.
4. Muller JG, Isomatsu Y, Koushik SV, O'Quinn M, Xu L, Kappler CS, Hapke E, Zile MR, Conway SJ, Menick DR. Cardiac-specific expression and hypertrophic upregulation of the feline Na(+)-Ca(2+) exchanger gene H1-promoter in a transgenic mouse model. *Circ Res.* 2002;90: 158-64.
5. Oka T, Xu J, Kaiser RA, Melendez J, Hambleton M, Sargent MA, Lorts A, Brunskill EW, Dorn GW, Conway SJ, Aronow BJ, Robbins J, Molkentin JD. Genetic Manipulation of Periostin Expression Reveals a Role in Cardiac Hypertrophy and Ventricular Remodeling. *Circ Res.* 2007;101:313-21.
6. Hirasawa M, Kitaura Y, Deguchi H, Ukimura A, Kawamura K. Spontaneous myocarditis in DBA/2 mice. Light microscopic study with transmission and X-ray analytical electron microscopic studies. *Virchows Arch.* 1998;432:461-8.
7. Norris R, Damon B, Mironov V, Kasyanov V, Ramamurthi R, Moreno-Rodriguez R, Trusk T, Potts J, Goodwin R, Davis J, Hoffman S, Wen X, Sugi Y, Kern K, Mjaatvedt C, Turner D, Oka T, Conway SJ, Molkentin J, Forgacs G, Markwald RR. Periostin regulates collagen fibrillogenesis and biomechanical properties of connective tissues. *JCB*, 2007;101:695-711.
8. Soonpaa M, Kim K, Pajak L, Franklin M, Field LJ. Cardiomyocyte DNA synthesis and binucleation during murine development. *Am J Physiol.* 1996;271:H2183-9.
9. Kanekar S, Borg TK, Terracio L, Carver W. Modulation of heart fibroblast migration and collagen gel contraction by IGF-I. *Cell Adhes Commun.* 2000;7:513-23.
10. Yang FC, Chen S, Clegg T, Li X, Morgan T, Estwick SA, Yuan J, Khalaf W, Burgin S, Travers J, Parada LF, Ingram DA, Clapp DW. Nf1+/- mast cells induce neurofibroma-like phenotypes through secreted TGF-beta signaling. *Hum Mol Genet.* 2006;15:2421-37.

11. Rios H, Koushik SV, Wang H, Wang J, Zhou HM, Lindsley A, Rogers R, Chen Z, Maeda M, Kruzynska-Frejtag A, Feng JQ, Conway SJ. Periostin null mice exhibit dwarfism, incisor enamel defects, and an early-onset periodontal disease-like phenotype. *Mol Cell Biol.* 2005;25:11131-44.
12. Rubart M, Pasumarthi KB, Nakajima H, Soonpaa MH, Nakajima HO, Field LJ. Physiological coupling of donor and host cardiomyocytes after cellular transplantation. *Circ Res.* 2003;92:1217-24.
13. Hinton RBJr, Lincoln J, Deutsch GH, Osinska H, Manning PB, Benson DW, Yutzey KE. Extracellular matrix remodeling and organization in developing and diseased aortic valves. *Circ Res.* 2006; 98:1431-8.
14. Kruithof BP, Krawitz SA, Gaussin V. Atrioventricular valve development during late embryonic and postnatal stages involves condensation and extracellular matrix remodeling. *Dev Biol*. 2007;302:208-17.
15. Borg TK, Rubin K, Lundgren E, Borg K, Obrink B. Recognition of extracellular matrix components by neonatal and adult cardiac myocytes. *Dev Biol* 1984;104:86-96.